JOURNAL OF MATERIALS SCIENCE 31 (1996) 2747–2755

Co-operative microbuckling of two fibres in a model composite

C. MUELLER, A. GORIUS*, S. NAZARENKO, A. HILTNER**, E. BAER
Department of Macromolecular Science and Center for Applied Polymer Research, Case Western Reserve University, Cleveland, OH 44106 USA

Cooperative fibre microbuckling, a compressive failure mechanism in unidirectional fibre-reinforced composites, was studied in a model system composed of two polyamide fibres in a transparent silicone matrix. The transparent matrix permitted direct observation of fibre microbuckling during compression. In all cases fibres buckled in a sinusoidal pattern with a critical wavelength characteristic of the fibre diameter and the modulus ratio of the fibre and matrix as observed previously with single fibre composites. At smaller separation distances, the two fibres microbuckled co-operatively in the common plane. At larger separation distances, the fibres microbuckled non-co-operatively in different planes. A stress overlap criterion based on the in-plane shear stress is proposed for co-operative fibre microbuckling.

1. Introduction

In compression, continuous fibre-reinforced composites often fail at a critical load by microbuckling [1, 2]. This instability limits the load carrying capacity of the system. Fibre microbuckling can also occur during high temperature curing if contraction of the matrix and fibres is significantly different [3, 4]. Fibre kinking, which is a shear failure mode of the fibre, may be closely related to fibre microbuckling. It has been suggested that kinks form in response to the bending strain in the microbuckled fibre [5]. It should be noted that microbuckling is not the same as Eulerian buckling, where an unsupported column under compressive load bows out as half a wave. Rather, for the case of microbuckling, the column is supported by a surrounding matrix or foundation and thereby buckles in many waves.

The mechanism of fibre microbuckling for a single fibre in an elastic matrix has been previously investigated [6]. It was found that the microbuckling occurs as a sinusoidal deformation of the fibre. The critical wavelength of fibre microbuckling was shown to be linearly dependent on the fibre diameter and dependent on the quarter power of the modulus ratio of the fibre and matrix as predicted by the analyses of Sadowsky *et al.* [7] and Darby and Kanellopoulos [8]. Single fibre studies do not address interactive effects between adjacent fibres as would be the case in a fibre-reinforced composite. Interactive effects are usually considered in terms of Rosen's [3] two-dimensional models for shear co-operative and transverse co-operative microbuckling modes. Attempts to test these two-dimensional models experimentally have confirmed only the shear co-operative mode [9].

The goal of this work was to investigate fibre interactions during microbuckling by synthesizing composites with two or three fibres. Use of a transparent, elastomeric matrix allowed direct observation of the fibres during compressive deformation. Different fibre volume fractions were simulated by varying the separation distance between the fibres.

2. Experimental procedure

2.1. Fabrication of the model composite

The model composite consisted of two polyamide monofilaments fibres aligned vertically within GE Silicones RTV 615, an optically clear elastomeric material. The mould used to prepare the composites consisted of a syringe cylinder or a segment of PVC pipe and a stopper for the bottom (Fig. 1). The fibre separation distance D and the parallel alignment of the fibres was controlled by looping the fibre around the rods that were inserted through the walls of the cylinder. To ensure good adhesion between fibre and matrix the fibre was treated with GE Silicones SS 4120 primer by dip-coating twice. The silicone matrix resin was thoroughly mixed with hardener in a 10:1 ratio and then placed in a vacuum to remove trapped air bubbles. The silicone was poured into the mould around a primed fibre which was held under enough tension to keep it straight along the central axis. The composite was cured at 100 °C for two hours.

* *Permanent address*: Rhone-Poulenc Fibres et Polymeres, 25 Quai Paul Doumer, 92408 Courbevoie, France.
** Authour to whom correspondence should be addressed.

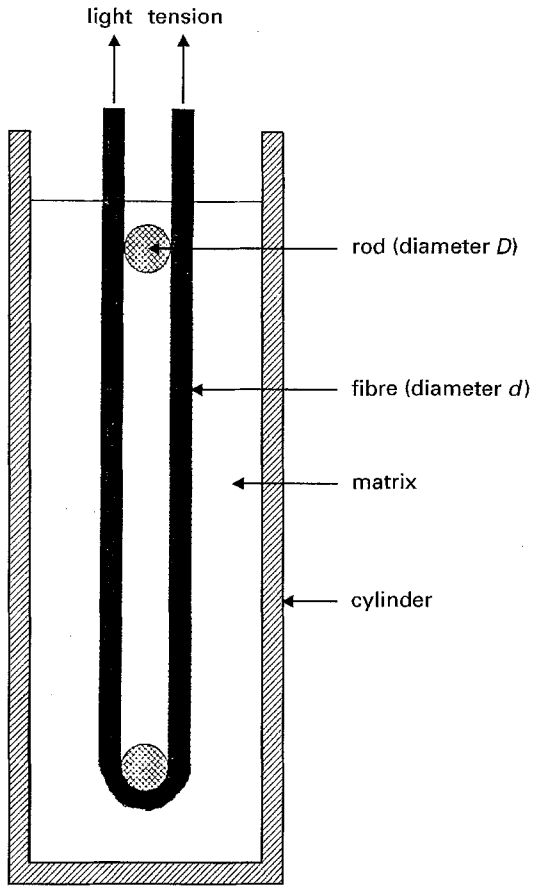

Figure 1 Sketch of the mould used to prepare composites with parallel fibres.

After curing, the composite was carefully removed from the mould, and the top and bottom faces were cut parallel to one another to ensure good alignment for compressive testing. To avoid edge effects, cylinder diameters of 2 and 4 cm were used so that the fibre was a minimum distance of twenty fibre diameters from the edge. In order to prevent Eulerian buckling of the entire composite cylinder, a length to diameter ratio of about 2.5 was maintained. Composites with three fibres in an equilateral triangular array were also prepared in the above manner. In this case, the fibres were held in place in the mould by stoppers in the top and bottom which had holes for each fibre.

2.2. Mechanical testing

All mechanical measurements were conducted with an Instron 1123 universal testing machine which was equipped with a compression fixture and an environmental chamber for temperature control. The modulus of the polyamide monofilaments was affected by the methanol and ethanol solvents of the primer solution. Consequently, in order to determine the true fibre modulus in the composite, monofilaments were primed, embedded in the silicone matrix and cured at 100 °C for two hours, then carefully removed from the matrix. The modulus of these fibres was determined in tension at a strain rate of 4% min^{-1}. The modulus of the transparent cured silicone rubber was determined in tension and compression at a strain rate of 1% min^{-1}. Fibre and matrix moduli were determined at temperatures ranging from -40 to 100 °C.

The composite samples, which were compressed to a maximum of 6% strain at a strain rate of 2% min^{-1}, were viewed from all sides by rotation of the compression fixture. Each sample was loaded in compression and unloaded twice to ensure that the microbuckling was reversible and reproducible. The tests were recorded with either a video or photographic camera arrangement. Strain fields around the buckled fibre were recorded at ambient temperature using a polarized light source and analyser. A Cue-4 image analysis system was used to analyse the photographic images obtained from the microbuckling tests.

3. Results and discussion

3.1. Compressive fibre microbuckling

The critical wavelength of the fibre at the instant of microbuckling, λ_0, was used to quantify the microbuckling. A unique λ_0 describes each combination of fibre diameter and ratio of fibre modulus to matrix modulus [6]. The fibre modulus, E_f, measured at various temperatures is given in Table I. It strongly depended on temperature, and increased about eightfold as the temperature decreased from 100 to -40 °C. Both the tensile and compressive moduli of the cured matrix elastomer were measured. They were identical up to 6% strain, the maximum used in this study. As expected for a cured rubber, the matrix modulus, E_m, decreased slightly as the temperature decreased from 100 to -40 °C as shown in Table I. The inverse temperature dependencies of fibre and matrix moduli produced a change in the modulus ratio, E_f/E_m, from about 2200 at -40 °C to 200 at 100 °C, a factor of 11 over a temperature range of 140 °C.

The sequence of fibre microbuckling for two parallel fibres is shown in Fig. 2. The first indication of microbuckling was the appearance of birefringence patterns around the fibres at about 1.5% compressive strain. Birefringence appeared around both fibres at the same instant indicating that they microbuckled simultaneously. Birefringence was only observed in the microbuckling plane where it extended outward from the fibre about six fibre diameters. The birefringence pattern did not grow in size as the amplitude of the waveform increased. At the initial stage of microbuckling, the amplitude of the waves was very small. With increasing compression, the amplitude increased, and it was possible to observe many waves along the fibres. When the load was removed the fibres returned to their original undeformed state. The pattern of the buckled fibres in all cases was identical to that of a single fibre as described previously [6]; that is, buckling occurred in a single plane and the microbuckling pattern was sinusoidal. The fibres in Fig. 2 both microbuckled in their common plane.

The critical wavelength of microbuckling, λ_0, i.e. the wavelength at the instant of microbuckling, was determined as in the previous study by averaging the pathlengths measured at several compressive strains. Definitions of the pathlength and λ_0 are shown

TABLE I Comparison of critical wavelength for co-operative fibre microbuckling and single fibre microbuckling

Temperature (°C)	E_f (MPa)	E_m (MPa)	E_f/E_m	λ_0/d One fibre	λ_0/d Two fibres	λ_0/d calc.[a]	λ_0/d calc.[b]
−40	2200	0.98	2250	20.4 ± 2.0	21.0 ± 1.7	19.1	19.4
0	1960	1.02	1920	17.4 ± 0.9	19.5 ± 3.5	18.4	18.4
25	1130	1.18	960	16.2 ± 0.9	13.8 ± 1.9	15.5	15.6
50	640	1.24	520	13.3 ± 0.5	10.3 ± 0.5	13.3	12.9

[a] Calculated using the Darby and Kanellopoulos [8] analysis.
[b] Calculated using the Sadowsky *et al.* [7] analysis.

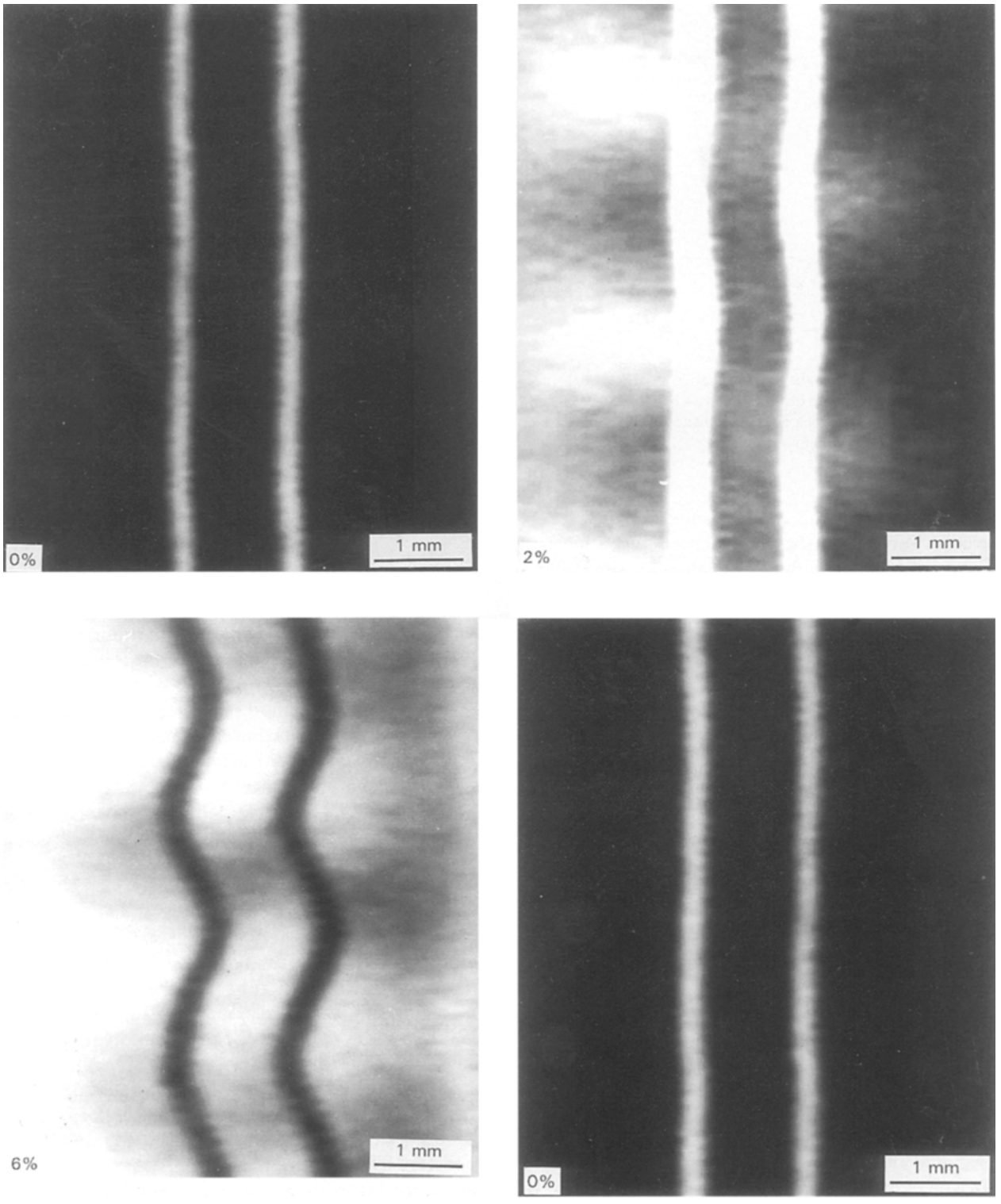

Figure 2 Sequence of fibre microbuckling for two parallel fibres with a separation distance $D/d = 4$ and a modulus ratio $E_f/E_m = 960$. The compressive strain is indicated.

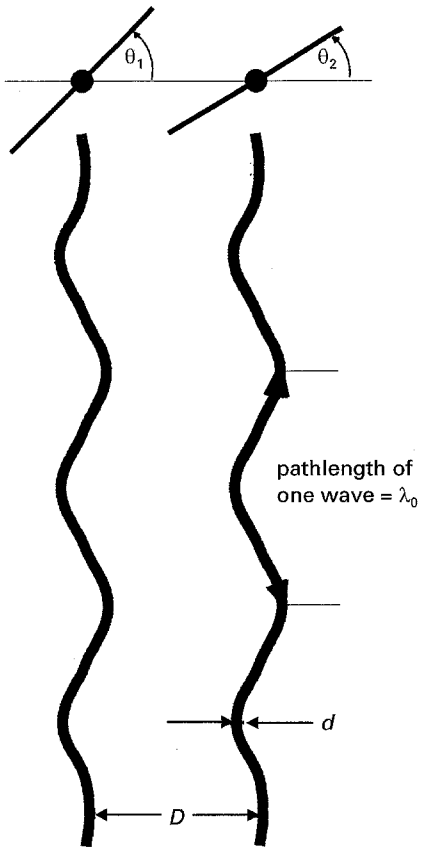

Figure 3 Sketch showing the fibre separation distance, D, the fibre diameter, d, the pathlength of a single wave which is equal to λ_0, and the angles, θ_1 and θ_2, which define the planes of the microbuckled fibres relative to their common plane.

schematically in Fig. 3, and measured values of λ_0 are given in Table II for the range of modulus ratios used in this study along with the λ_0 values for single fibres from the previous study. The measured values of λ_0 are very similar for single fibres and two fibres. This indicates that microbuckling of two fibres also follows the analysis of Sadowsky *et al.* [7] which has been simplified by Darby and Kanellopoulos [8] to

$$\lambda_0 = \pi d \left(\frac{E_f^2}{8 G_m E_m} \right)^{1/8} \quad (1)$$

where G_m is the matrix shear modulus and d the fibre diameter. This equation applies only for large modulus ratios.

Composites with separation distances ranging from three to twenty fibre diameters were tested. Fibres that were close together were observed to microbuckle in the same plane; fibres that were farther apart microbuckled in different planes. The wave patterns of the two fibres were always in phase as expected from the identical boundary conditions. The angles of the microbuckling planes with the common plane, θ_1 and θ_2, defined in Fig. 3, were used to differentiate the modes of microbuckling. Fibres that were relatively close to one another were observed to microbuckle in the same plane ($\theta_1 = \theta_2 = 0°$) as shown in Fig. 4. Microbuckling in the same plane is defined as co-operative microbuckling. At larger separation distances the fibres microbuckled in different planes as shown in Fig. 5. The microbuckling is defined as non-co-operative if both fibres microbuckle out of the common plane. The transition between the two microbuckling modes occurred at fibre separation distances of about 10 or 11 fibre diameters for the modulus ratio of 960. A number of samples were tested at these separation distances and both co-operative and non-co-operative microbuckling were observed along with intermediate transitional behaviour. This latter was marked by one fibre microbuckling in the common plane and the other fibre microbuckling slightly out of the common plane ($\theta_1 = 0°$ and $\theta_2 = 10$ to $20°$). These results are compiled in Table II for composites with a modulus ratio of 960.

TABLE II Observed microbuckling mode as a function of fibre separation

Fibre separation (D/d)	Number of specimens	θ_1 (degrees)	θ_2 (degrees)	Mode
3	1	0	0	co-operative
4	1	0	0	co-operative
4.5	1	0	0	co-operative
5	1	0	0	co-operative
6	1	0	0	co-operative
7.5	1	0	0	co-operative
8	1	0	0	co-operative
8.5	1	0	0	co-operative
10	5	0	0	co-operative
	1	0	15	transitional
11	2	0	0	co-operative
	1	0	10	transitional
	1	0	15	transitional
	1	40	80	non-co-operative
	1	60	80	non-co-operative
15	1	40	45	non-co-operative
20	1	30	45	non-co-operative
	1	40	45	non-co-operative
	1	50	90	non-co-operative
	1	20	135	non-co-operative

TABLE III Microbuckling of two fibres with different diameters

d_1 (mm)	d_2 (mm)	D (mm)	θ_1	θ_2
0.21	0.30	1.28	10	50
0.21	0.30	1.80	0	75
0.23	0.32	3.22	60	15
0.21	0.30	3.22	45	15

Composites with modulus ratios of 960 were prepared with two fibres of different diameters, d_1 and d_2, and fibre separation distances as shown in Table III. When compressed, each fibre microbuckled in a different plane with its own characteristic λ_0; the observed values being in agreement with Equation 1. This occurred even when the fibres were relatively close to each other. A triangular array of three identical fibres was also tested. The fibres in this composite were arranged in an equilateral triangle with the fibres separated from one another by a distance of five fibre diameters. Fig. 6 shows the microbuckling behaviour of this composite. It is nearly equivalent to that of the two fibres that microbuckled co-operatively. The fibres buckled in phase with each other, and the

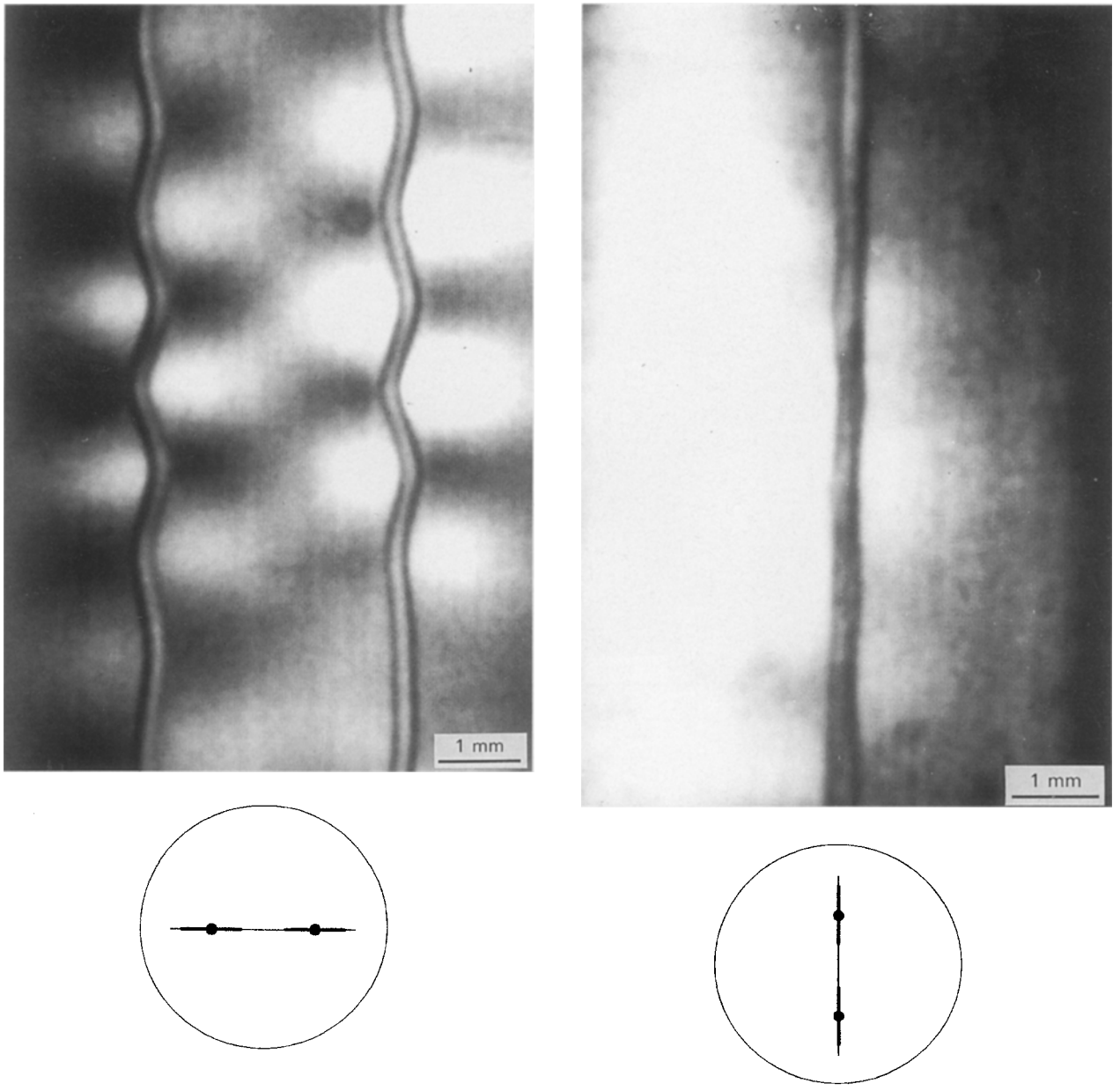

Figure 4 Two-fibre composite with a modulus ratio $E_f/E_m = 960$ under crossed polarizers at 6% remote compression showing co-operative microbuckling for $D/d = 8$ with $\theta_1 = \theta_2 = 0°$. The schematics indicate the orientations of the microbuckling planes and the common plane. The co-operative microbuckling was viewed perpendicular and parallel to the common plane.

microbuckling planes of the fibres were nearly parallel to one another with two fibres in their common plane and the other in a parallel plane. This type of behaviour for a three-dimensional array was also observed by Dale and Baer [4].

3.2. Models for co-operative microbuckling

Historically, microbuckling of two or more fibres in composite has been discussed in the manner proposed by Rosen [3]. This two-dimensional model considers the two modes of co-operative microbuckling shown schematically in Fig. 7. The shear co-operative mode has the waves aligned, or in phase, with one another, and the transverse co-operative mode has the waves out of phase with one another. By comparing the compressive strength associated with each mode, the preferred mode at a given fibre separation can be determined. The shear co-operative mode compressive strength ($\sigma_{c,s}$) is

$$\sigma_{c,s} = \frac{(d + D)\, G_m}{D} \tag{2}$$

and the transverse cooperative mode compressive strength ($\sigma_{c,t}$) is

$$\sigma_{c,t} = \frac{2d}{d + D}\left(\frac{d\, E_m\, E_t}{3D}\right)^{1/2} \tag{3}$$

Qualitatively it can be seen that the shear mode should dominate at small fibre separation distances, while the transverse mode should be preferred at large fibre separation distances. Using the modulus values for the polyamide fibre and silicone matrix, the compressive strength as a function of reduced fibre separation distance, D/d, was calculated for the two modes. The results are plotted in Fig. 8. If only these two

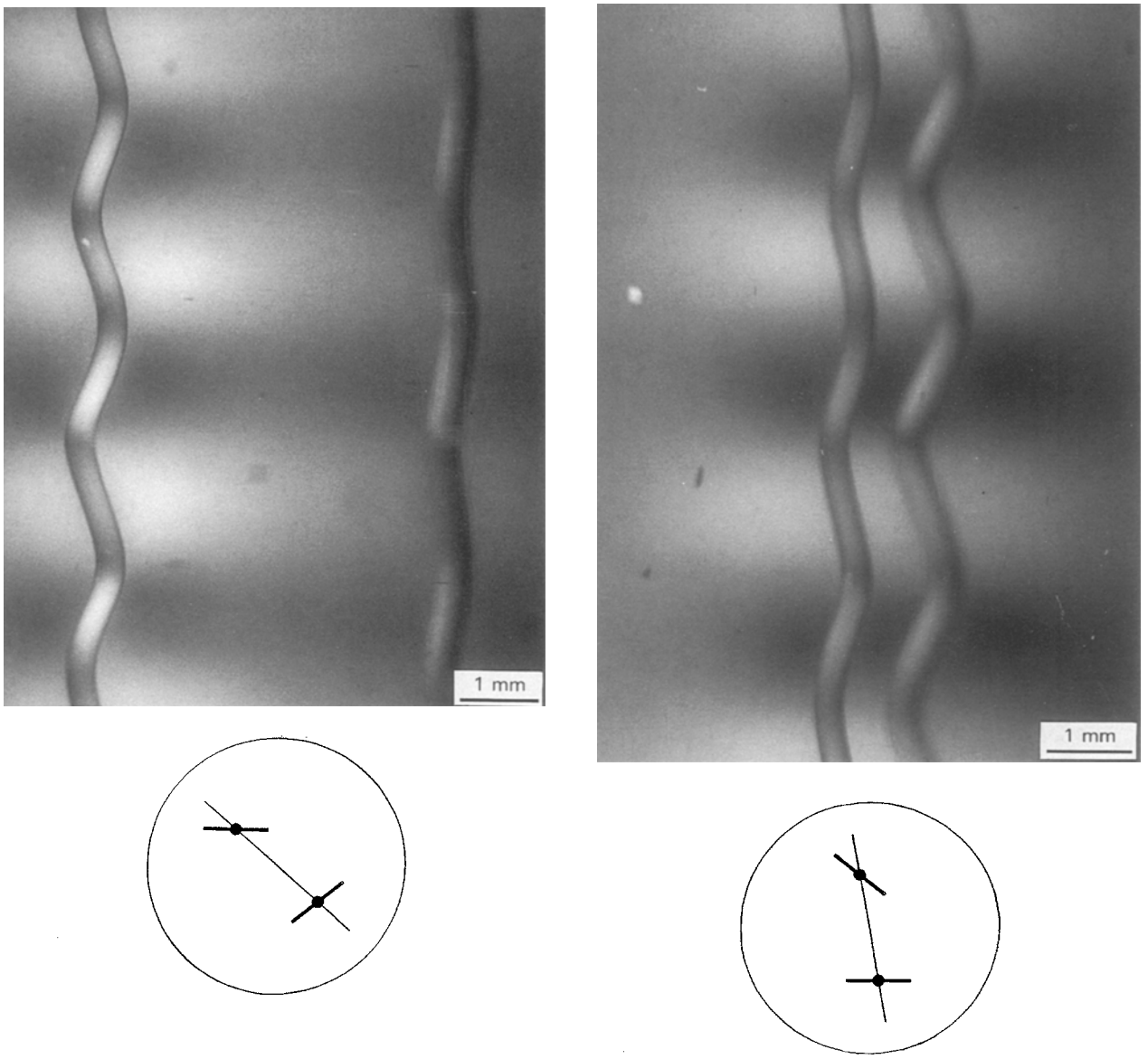

Figure 5 Two-fibre composite with a modulus ratio $E_f/E_m = 960$ under crossed polarizers at 6% remote compression showing non-co-operative fibre microbuckling for $D/d = 11$ with $\theta_1 = 40°$ and $\theta_2 = 80°$. The non-co-operative microbuckling was viewed perpendicular to one or the other of the microbuckling planes.

modes are considered, the transition from the shear mode to the transverse mode is predicted at a fibre separation distance of about 21 fibre diameters. The experimental observations show co-operative microbuckling equivalent to the shear mode at smaller fibre separations, as predicted. However, at a separation distance of 10–11 fibre diameters there is a transition to non-co-operative microbuckling, and the transverse mode is never observed. Rosen's model does not address non-co-operative microbuckling.

A stress overlap criterion is proposed for the transition from co-operative to non-co-operative microbuckling. It is assumed that fibres microbuckle co-operatively when the stresses generated by the microbuckling fibres overlap sufficiently. Consider two identical fibres infinitely far apart in a matrix and apply remote compression to them. For a given set of material properties, λ_0 is uniquely defined, for example by the equations of Darby and Kanellopoulos [8] and Sadowsky *et al.* [7] so the wavelength must be the same for both fibres. Furthermore, because the boundary conditions are identical the two fibres microbuckle in phase. If there is no interaction between the two fibres, the probability that they microbuckle in different planes is much greater than the probability that they microbuckle in their common plane. Each of the fibres generates a three-dimensional stress field in the matrix as it microbuckles; the stress fields can interact if the fibres are close enough together. It is hypothesized that when this occurs, the configuration corresponding to the energy minimum will be co-operative microbuckling in the common plane. It follows that the controlling stress component is the in-plane shear stress, τ_{xz}, in the coordinate system shown schematically in Fig. 9.

The stress overlap between two fibres can be characterized by the stress at the midpoint between the two fibres because of the symmetry of the stress distribution. As a consequence, the stress overlap criterion

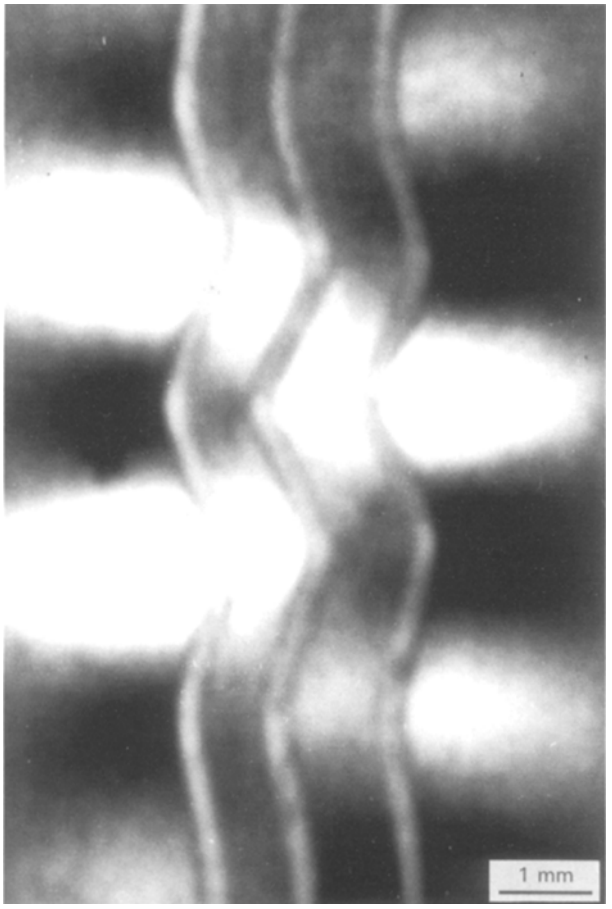

Figure 6 Co-operative fibre microbuckling in a composite with three fibres in a triangular array. The modulus ratio was $E_f/E_m = 960$ and the strain was 6% remote compression.

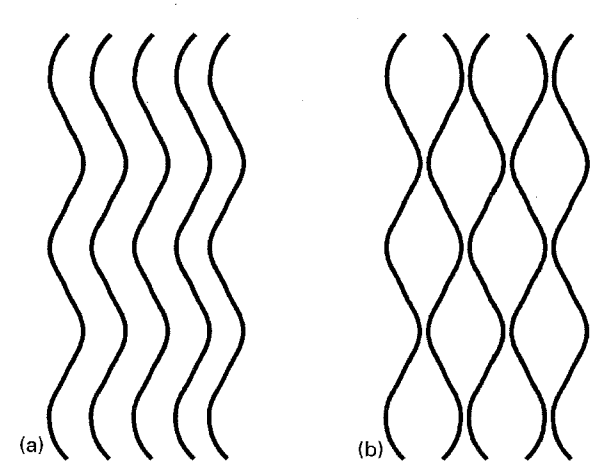

Figure 7 Sketches of Rosen's proposed two-dimensional microbuckling modes [3]: (a) shear co-operative and (b) transverse co-operative.

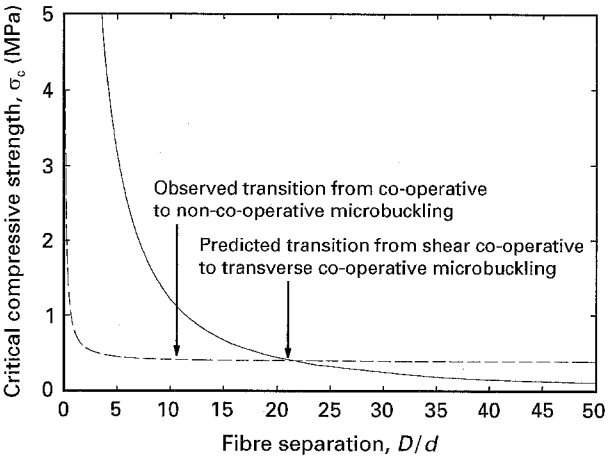

Figure 8 Calculated compressive strength as a function of fibre separation for Rosen's shear co-operative (- - -) and transverse co-operative (—) modes for a composite with modulus ratio $E_f/E_m = 960$.

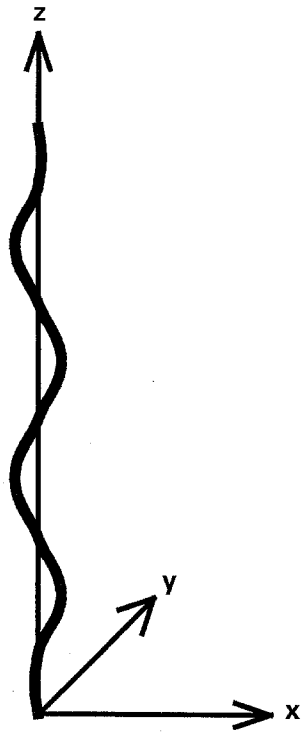

Figure 9 Coordinate system used to calculate stresses in the matrix surrounding the fibre. The fibre is oriented along the z-axis and the microbuckling plane is the xz plane.

for cooperative microbuckling can be stated as

$$\frac{\text{amplitude of stress at mid-distance}}{\text{amplitude of stress at fibre surface}} = k \quad (4)$$

where k is some constant which takes the critical value k^* at the transition. For a given k, Equation 4 is an implicit relationship between D/d and the material properties. From the experimental observations for our system, it is seen that the transition from co-operative to non-co-operative microbuckling occurs at large D^*/d, the critical fibre separation distance normalized to the fibre diameter. In this limit, the only length scale involved in the system is λ_0 so that the stresses at any given distance D from one fibre are a function of D/λ_0 only. Thus the k^* criterion

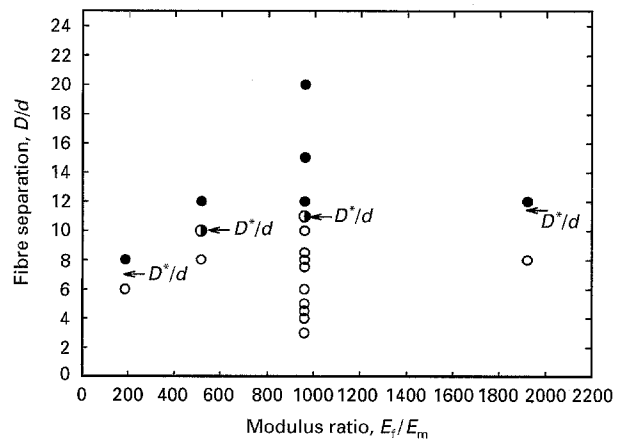

Figure 10 Effect of modulus ratio, E_f/E_m, and fibre separation, D/d, on microbuckling mode. ● non-co-operative; ◑ transition; ○ co-operative.

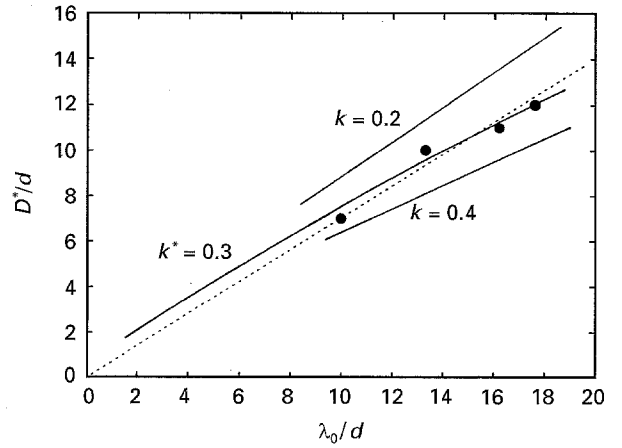

Figure 11 Fit of stress overlap criterion for the transition from co-operative to non-co-operative microbuckling to the experimental data. The dashed line indicates the scaling law which passes through the origin.

translates into a proportionality between D^* and λ_0. By changing the test temperature, values of D^*/d were obtained for four modulus ratios as in Fig. 10. At the large modulus ratios of this system, D^* appears to scale with λ_0 as indicated by the line which passes through the origin (Fig. 11).

However, to fully define the dependency of D^* on the modulus ratio for all cases, it is necessary to consider the full stress distribution around the fibre at the instability threshold. Using the results of Sadowsky *et al.* [7], the amplitudes of the stresses at the moment of the microbuckling instability were calculated numerically as a function of location and material properties. The calculated distribution for the in-plane shear stress, τ_{xz}, from a single fibre at distances of $r = 3d$, $6d$ and $12d$ is shown in Fig. 12(a) for a modulus ratio of 960. This is compared with the out-of-plane shear stress, τ_{yx}, in Fig. 12(b) at the same distances. The out-of-plane shear stress is very small compared to the in-plane shear stress. Observation of birefringence only in the in-plane direction and not in the out-of-plane direction is consistent with these calculations. The in-plane compressive stress, σ_z, is given in Fig. 12(c). In contrast to the in-plane shear stress,

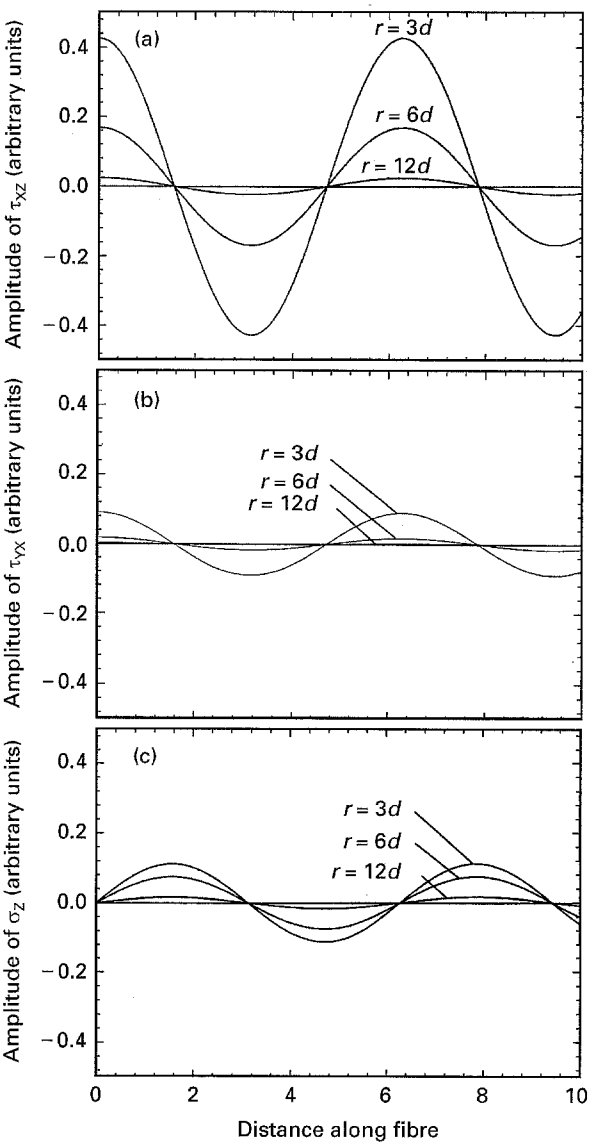

Figure 12 Calculations of the amplitudes of the stresses around a fibre at the moment of the instability for a modulus ratio $E_f/E_m = 960$ at various distances r from the fibre: (a) the in-plane shear stress τ_{xz}, (b) the out-of-plane shear stress τ_{yx}, and (c) the in-plane tensile–compressive stress σ_z.

σ_z is much smaller in magnitude and does not change rapidly with distance from the fibre. These comparisons of the stresses at the moment of microbuckling indicate that the in-plane shear stress plays a key role in determining the stress overlap criterion for co-operative fibre microbuckling. This conclusion is supported by the appearance of overlapping birefringence patterns in the common plane as the first indication of co-operative microbuckling.

Within the limits of linear elastic theory, it is possible to add the τ_{xz} stress tensors generated by the two fibres and to calculate k^* numerically from experimental D^*/d values. This procedure gave an average value of $k^* = 0.3$. This result was found to be insensitive to Poisson's ratio, ν, for both fibre and matrix. In all reported calculations a value of $\nu = 0.33$ was used. To demonstrate the sensitivity of k^*, the experimental data are compared with calculations for three values of k in Fig. 11. In this range of large λ_0, the relationship between D^* and λ_0 is nearly linear for a given k.

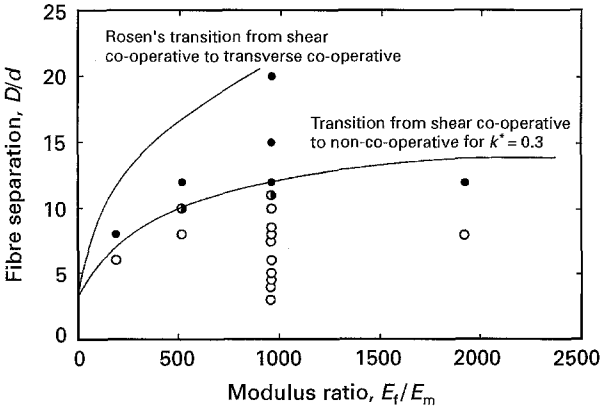

Figure 13 Stability map with the co-operative to non-co-operative microbuckling transition predicted by the stress overlap criterion with $k^* = 0.3$ and Rosen's predicted shear co-operative to transverse co-operative microbuckling transition. ● non-co-operative; ◑ transition; ○ co-operative.

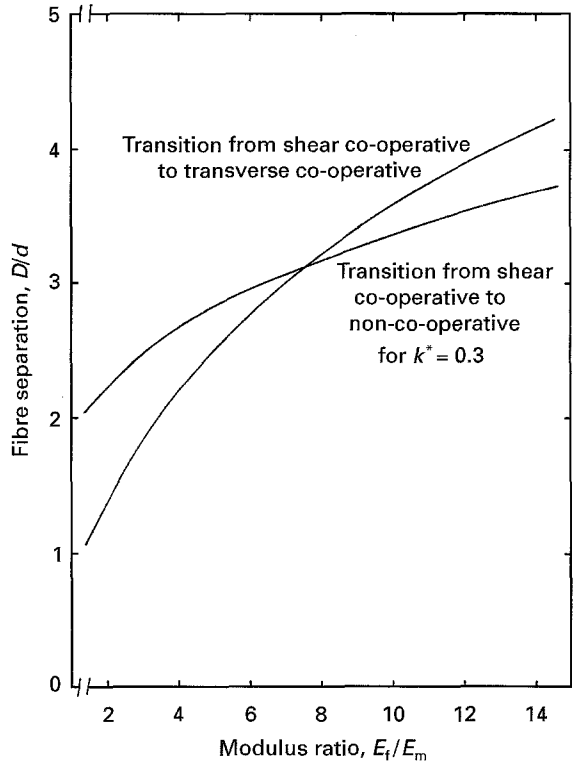

Figure 14 Stability map at low modulus ratios where transverse co-operative microbuckling may be possible.

Non-linearity at smaller λ_0 is shown by the extension of the $k^* = 0.3$ curve in Fig. 11. Although the value of $k^* = 0.3$ fits the data well, the scaling relationship shown by the dashed line provides an excellent approximation for predicting D^* from λ_0 without the need for lengthy calculations of the shear stress.

According to this stress overlap criterion with $k^* = 0.3$ the transition from co-operative to non-co-operative microbuckling as a function of modulus ratio can be predicted by calculating for a given system D^*/d as a function of modulus ratio, E_f/E_m. Considering again Rosen's predicted transition from shear co-operative to transverse co-operative microbuckling, a stability map that incorporates all three modes can be constructed as shown in Fig. 13. When the co-operative to non-co-operative microbuckling transition is compared with the predicted transition from shear co-operative to transverse co-operative microbuckling, it is evident that non-co-operative microbuckling occurs before the predicted transition to transverse co-operative microbuckling. Even though the linearity assumptions may break down at low modulus ratios, extrapolation to this regime suggests that the transition from shear co-operative to transverse co-operative mode would be observed only at very low E_f/E_m ratios where D^* is very small, as shown in Fig. 14. This would require very special and unusual circumstances.

4. Summary

A three-dimensional composite with two fibres in a transparent, elastomeric matrix permitted observation of fibre microbuckling during compressive deformation. The microbuckling of the fibres was sinusoidal, and had a unique λ_0 characteristic of the fibre diameter and the modulus ratio of the fibre and matrix. Both co-operative and non-co-operative microbuckling modes were observed as a function of the fibre separation distance. It was proposed that co-operative microbuckling is governed by interaction of the in-plane shear stress fields surrounding the fibres. This formed the basis of a stress overlap criterion for the transition from co-operative to non-co-operative microbuckling.

Acknowledgements

This research was supported in part by the Army Research Office, Grant DAAL03-92-G-0241. One of the authors (AG) gratefully acknowledges the financial support provided by Rhone-Poulenc Fibres et Polymeres SA. Special thanks to Mohd Mat Raschid for help in sample preparation and testing.

References

1. F. CHEN, S. BAZHENOV, A. HILTNER and E. BAER, *Composites* **25** (1994) 11.
2. *Idem., ibid.* **25** (1994) 21.
3. B. W. ROSEN, in "Fiber composites" (ASM, Metals Park, Ohio, 1965) p. 37.
4. W. C. DALE and E. BAER, *J. Mater. Sci.* **9** (1974) 369.
5. A. S. ARGON, in "Treatise on materials science and technology," Vol. 1, edited by H. Liebowitz (Academic Press, New York, 1972) p. 106.
6. C. MUELLER, A. GORIUS, S. NAZARENKO, A. HILTNER and E. BAER, *J. Comp. Mater.* in press.
7. M. A. SADOWSKY, S. L. PU and M. A. HUSSAIN, *J. Appl. Mech.* **34** (1967) 1011.
8. M. I. DARBY and V. N. KANELLOPOULOS, *J. Phys. D: Appl. Phys.* **20** (1987) 298.
9. W. Y. CHUNG and R. B. TESTA, *J. Comp. Mater.* **3** (1968) 58.

Received 30 August
and accepted 4 October 1995